ACS OMEGA

http://pubs.acs.org/journal/acsodf

Article

Highly Efficient Uptake of TcO_4^- by Imidazolium-Functionalized Wood Sawdust

Fangfei Dong, Xiaomin Li, Yiwei Huang, Xupeng Zhi, Suliang Yang,* and Yinglin Shen*

Cite This: *ACS Omega* 2021, 6, 25672−25679

Read Online

ACCESS | Metrics & More | Article Recommendations | Supporting Information

ABSTRACT: ^{99}Tc is a radioactive fission product, mainly in the form of TcO_4^-, with good solubility and mobility in the environment. The development of effective and inexpensive materials to remove TcO_4^- from nuclear industry wastewater or contaminated water is significant. Wood sawdust is a byproduct of the wood processing industry and is an abundant, low-cost, and sustainable material. The mesostructure of wood consists of numerous hollow cells that are joined endwise to form an interconnected channel matrix capable of rapid transfer of ions. Imidazolium-functionalized wood sawdust (IM-WS) was synthesized using natural wood sawdust by a two-step reaction. It has excellent properties of TcO_4^-/ReO_4^- adsorption including rapid adsorption dynamics (30 s to equilibrium), good adsorption stability (pH 3−9), high selectivity (adsorption of 45.4 Re % in 1000 times excess of NO_3^- ions, 76.6 Re % in 6000 times excess of SO_4^{2-} ions, and 92.2 Tc % in a simulated mixed solution; after adsorption, the concentration of TcO_4^- decreased to 0.056 ppb from the initial concentration of 12.09 ppb in 1000 times excess of SO_4^{2-}), and in particular low production costs. These characteristics give it great prospects for low-level radioactive wastewater treatment and environmental remediation.

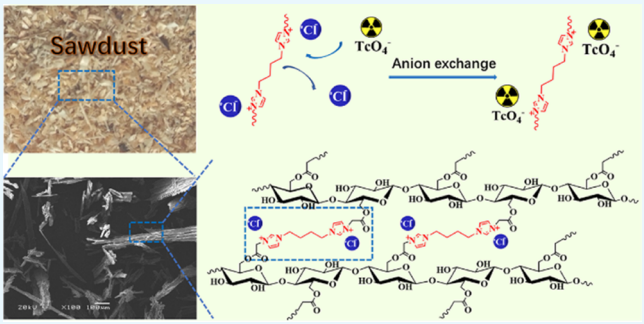

1. INTRODUCTION

Technetium-99 (^{99}Tc) is produced from fission of ^{235}U and ^{239}Pu with a high yield (≈6.1%) in a nuclear reaction.[1,2] ^{99}Tc has a half-life of 2.1×10^5 years and is a weak β emitter with a maximum energy of 0.29 MeV.[3] When exposed to the environment, it exists as the pertechnetate anion (TcO_4^-). Due to the high solubility and mobility of TcO_4^- underground, it needs more attention than other radionuclides.[4,5]

There are two general strategies to remove pertechnetate from the environment. One is by reducing the $Tc(VII)O_4^-$ anion to less soluble technetium oxides $Tc(IV)O_2$ and then sequestering it.[5−8] Fe(II),[5−7,9] sulfides, and iron sulfides[10−12] have been employed for the reduction of TcO_4^-, but it is difficult to prevent Tc(IV) from re-oxidation during the long geological disposal period.[13] The other effective strategy is using ion exchange, extraction, and gravity precipitation to capture TcO_4^-.[14−17] Ion exchange is considered to be a promising method with the advantages of easy implementation and high efficiency.[18]

In the last few decades, several types of polyionic materials have been studied to dispose off TcO_4^-.[18−20] Ion-exchange resins show slow kinetics and poor selectivity when taking up TcO_4^-.[21] Inorganic cationic materials, such as layered double hydroxides (LDHs),[22] LRHs,[23] and NDTB-1,[19] are easy to synthesize but have low sorption capacity and poor selectivity toward TcO_4^-. The designed and synthesized cationic metal−organic frameworks (MOFs),[13,24,25] covalent organic frameworks (COFs),[26,27] nanomaterials,[28] and porous organic polymers (POPs)[29] can selectively and rapidly adsorb TcO_4^-, but they suffer from high costs.

The recently reported imidazolium polymer SCU-CPN-1[30] and imidazolium porous organic polymer ImPOP-1[29] show excellent adsorption capacity and extraordinary selectivity to TcO_4^-. It is proved that the imidazolium cation is the key part for highly selective adsorption of TcO_4^-.

Wood, a natural three-dimensional (3D) porous material, has the advantages of renewable, sustainable, and abundant resources. Due to the internal micropores and microchannels, it has more opportunities to contact pollutants in water. Wood-functionalized materials have become one of the most promising candidates for wastewater treatment. UiO-66/wood,[31] Mn_3O_4/TiO_2/wood,[32] Pd NPs/wood,[33] and β-CD/WS[34] have been reported to remove organic pollutants (e.g., methylene blue, rhodamine 6G, and propranolol) from aqueous solutions. LS-C_3N_4/CWS[35] and SH-wood[36] show

Received: July 16, 2021
Accepted: September 9, 2021
Published: September 23, 2021

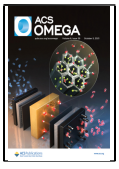

Scheme 1. Synthesis Route to IM-WS

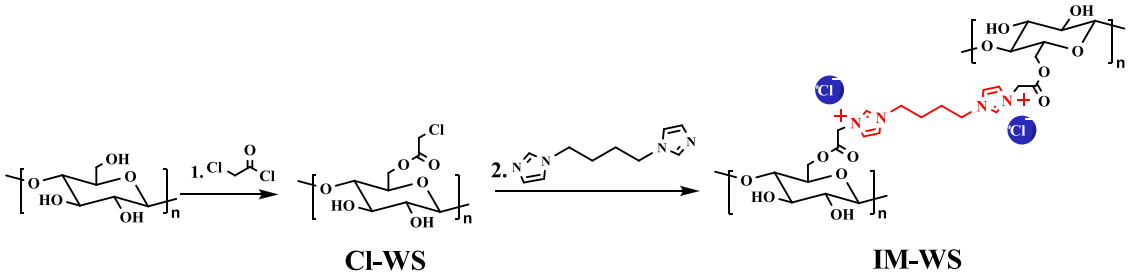

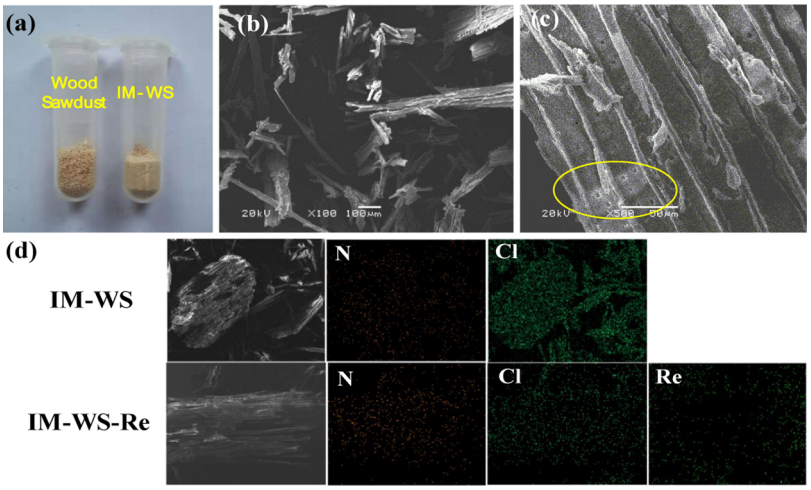

Figure 1. (a) Picture of the natural wood sawdust and IM-WS. (b) Scanning electron microscopy (SEM) image showing the microchannels of IM-WS. (c) Magnified SEM image showing numerous micropores of IM-WS. (d) Energy-dispersive spectrometry (EDS) mapping of IM-WS and IM-WS-Re.

excellent decontamination capability toward Pb^{2+}, Cd^{2+}, and Cu^{2+}.

In this work, wood chips and sawdust are chosen as the matrix material due to their natural wood properties and low cost, which are byproducts of the wood processing industry.[34] Imidazolium-functionalized wood sawdust (IM-WS) was synthesized by grafting 1,1′-(1,4-butanediyl)diimidazole groups on the cellulose of natural wood sawdust. Up to now, there have been no imidazolium-based biomass materials reported for the treatment of TcO_4^-. The interconnected network structure in natural wood sawdust and imidazolium cations enables effective removal of TcO_4^-.

Herein, we evaluated the removal capability of IM-WS for TcO_4^-/ReO_4^- by a batch adsorption experiment. In most experiments, ReO_4^- was used as the surrogate of radioactive TcO_4^- given their almost identical charge densities and similar chemical behaviors.[16]

2. RESULTS AND DISCUSSION

2.1. Synthesis and Characterization of IM-WS. Wood sawdust or wood chips, a natural material, are cheap and mechanically stable and can be processed into different shapes and sizes. The cellulose of wood sawdust (about 40−45%) has a large number of modifiable hydroxyl groups, which makes it a good graft matrix material.

The imidazolium-functionalized wood sawdust was synthesized by a two-step reaction, shown as Scheme 1. Natural wood sawdust reacted with chloroacetyl chloride to form esterification products, which via quaternization with 1,1′-(1,4-butanediyl)diimidazole afforded the final product. It can be seen from Figure 1a that the modified sawdust becomes smaller due to stirring for a long time.

The successful grafting of the imidazolium cation is confirmed by elemental analysis, scanning electron microscopy (SEM), energy-dispersive spectrometry (EDS), and Fourier transform infrared spectroscopy (FT-IR). Elemental analysis reveals a nitrogen content of 2.59 wt % (Table S1), corresponding to 0.27 mmol g^{-1} imidazolium cation in IM-WS. Scanning electron microscopy (SEM) images of IM-WS (Figure 1b,c) show that the sawn-off vessel channels and micropores are well maintained after functionalization. The sawn-off vessel channels, the micropores, the natural 3D structure of wood sawdust, and grafted imidazolium make IM-WS an ideal material for ion exchange. The energy-dispersive spectrometry (EDS) mappings of IM-WS exhibit distribution of Cl and N elements throughout the material (Figure 1d). In contrast, there are no chlorine and nitrogen in natural wood sawdust (Figure S1). The elemental distribution mappings prove that the cellulose is grafted with the imidazolium cation uniformly.

On comparison of the FT-IR spectra of IM-WS with those of natural wood sawdust (WS), many new peaks appear (Figure 2). The peak at 1753 cm^{-1} is attributed to the C═O stretching vibrations of the −COO− bond. The characteristic absorption peak of the imidazolium cation appears at 1100 cm^{-1}. The peaks at 1568 and 1627 cm^{-1} correspond to the vibration of the imidazole ring skeleton. The peak at 2963 cm^{-1} is attributed to the C−H stretching vibrations of $-CH_2-$ bonds of 1,1′-(1,4-butanediyl)diimidazole. All of these findings indicate the successful synthesis of IM-WS.

https://doi.org/10.1021/acsomega.1c03784
ACS Omega 2021, 6, 25672−25679

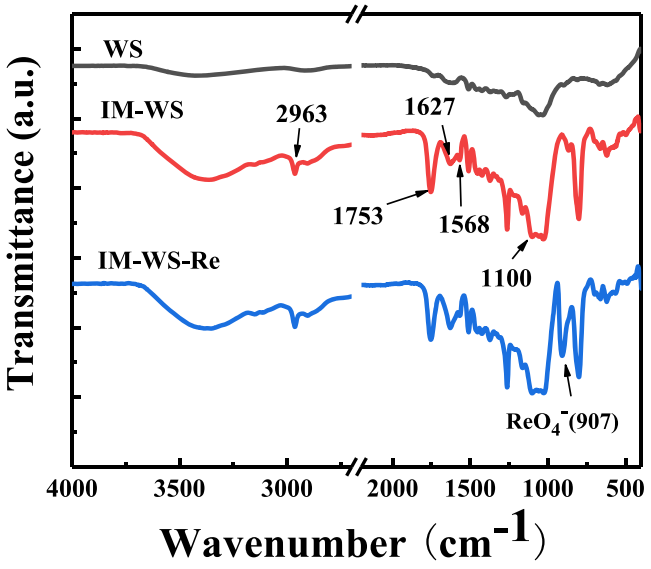

Figure 2. FT-IR spectra of WS, IM-WS, and IM-WS-Re.

2.2. ReO_4^-/TcO_4^- Adsorption. *2.2.1. Sorption Kinetics.* To evaluate the IM-WS adsorption performance toward TcO_4^-, a series of adsorption experiments were carried out. IM-WS (10 mg) was added to 5 mL of an aqueous solution containing 100 ppm ReO_4^- in the designed time for studying the sorption kinetics of IM-WS. As shown in Figure 3a, the adsorption achieved equilibrium within 30 s. The distribution coefficient (K_d) was calculated using the following equation

$$K_d = \left(\frac{C_0 - C_e}{C_e}\right)\frac{V}{m} \quad (1)$$

where C_0 and C_e are the concentrations of ReO_4^- solution (mg L^{-1}) initially and at equilibrium, respectively, m is the mass of the absorbent (g), and V is the volume of the solution (L). The K_d value is an important parameter that can reflect the affinity and selectivity of the adsorbents. The K_d of IM-WS toward ReO_4^- reaches an outstanding value of 3.79×10^5 mL g^{-1}, which is a competitive value among the materials reported so far (Table 1). The excellent adsorption rate of IM-WS on ReO_4^- is conducive to the rapid reduction of pollution by radioactive Tc, making IM-WS an attractive environmental remediation material, which can effectively remove Tc released into the environment. The absorption kinetics data are fitted with pseudo-first-order and pseudo-second-order kinetic models. On comparing the correlation coefficients (R^2) of these two models (Table S2), the adsorption process is more in line with the pseudo-second-order kinetic model with a high R^2 of 1 (Figure 3b). It can be considered that the adsorption process is chemical homogeneous adsorption.

Table 1. Comparison of the Distribution Coefficient (K_d) by Cationic Materials

cationic materials		K_d (mL g^{-1})	solid/liquid ratio (g L^{-1})	ref
inorganic materials	$Y_2(OH)_5Cl$	112	0.5	13
	$Yb_3O(OH)_6Cl$	120	0.5	13
	Mg-Al-LDH	262	1	24
ion-exchange resins	Purolite A-850	102		37
	Purolite A 532E	1.28×10^4		37
MOF materials	SCU-100	3.3×10^5	1	24
	SCU-101	7.5×10^5	1	38
	SCU-102	5.6×10^5	10	39
	SCU-103	$>1.00 \times 10^5$	1	40
COF materials	SCU-COF-1	3.89×10^5	1	27
POP materials	PQA-*p*N(Me)2Py-Cl	1.00×10^7	1	41
imidazolium-based organic polymer materials	ImPOP-1	3.2×10^5	0.5	29
	IM-WS	**3.79×10^5**	2	**this work**
	SCU-CPN-1	6.2×10^5	1	30

2.2.2. Sorption Isotherm Tests. To investigate the saturated adsorption capacity of IM-WS toward ReO_4^-, 10 mg of IM-WS was added to 5 mL of ReO_4^- aqueous solution. The initial concentrations of ReO_4^- were varied from 100 to 1500 ppm.

The adsorption isotherm data were fitted with the Langmuir and Freundlich sorption isotherm models. As shown in Figure 4a,b, the Langmuir model fits the equilibrium adsorption process well with a high correlation coefficient R^2 of 0.9994, which means that the IM-WS can take up ReO_4^- efficiently by monolayer adsorption. The theoretical sorption capacity q_{max} (201.2 mg g^{-1}) calculated by the Langmuir model is very close to the experimental value of 200.1 mg g^{-1}.

2.2.3. Adsorption Mechanism Study. The adsorption process of IM-WS toward Re was studied by determining the composition of the material after adsorption. Typically, 30 mg of IM-WS was added to 15 mL of an aqueous solution containing 1500 ppm ReO_4^-, whose pH was adjusted to 7. The mixture was stirred at 25 °C for 12 h, and then the Re-loaded

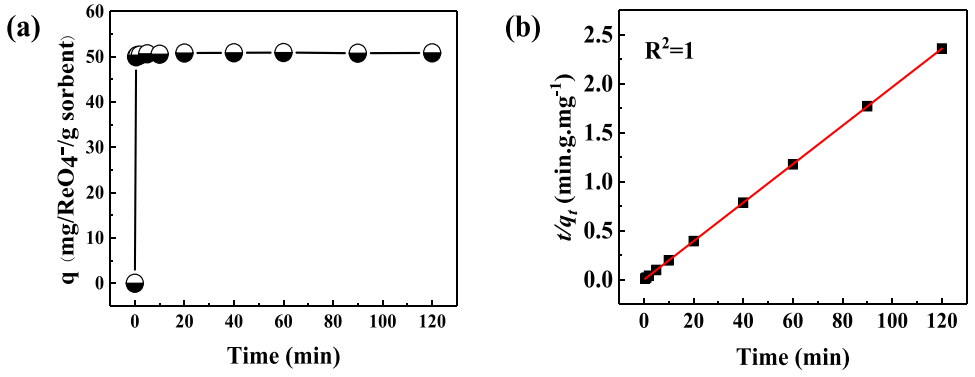

Figure 3. (a) ReO_4^- sorption kinetics of IM-WS under the ReO_4^- initial concentration of 100 ppm with the m/V ratio at 2 g L^{-1}. (b) Pseudo-second-order kinetic plot for adsorption.

https://doi.org/10.1021/acsomega.1c03784
ACS Omega 2021, 6, 25672−25679

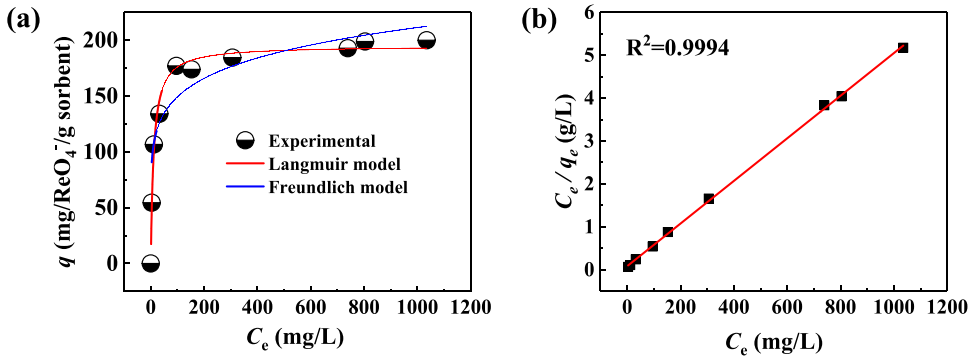

Figure 4. (a) ReO_4^- adsorption isotherm for IM-WS. (b) Linear regression by fitting the equilibrium adsorption data with the Langmuir adsorption model.

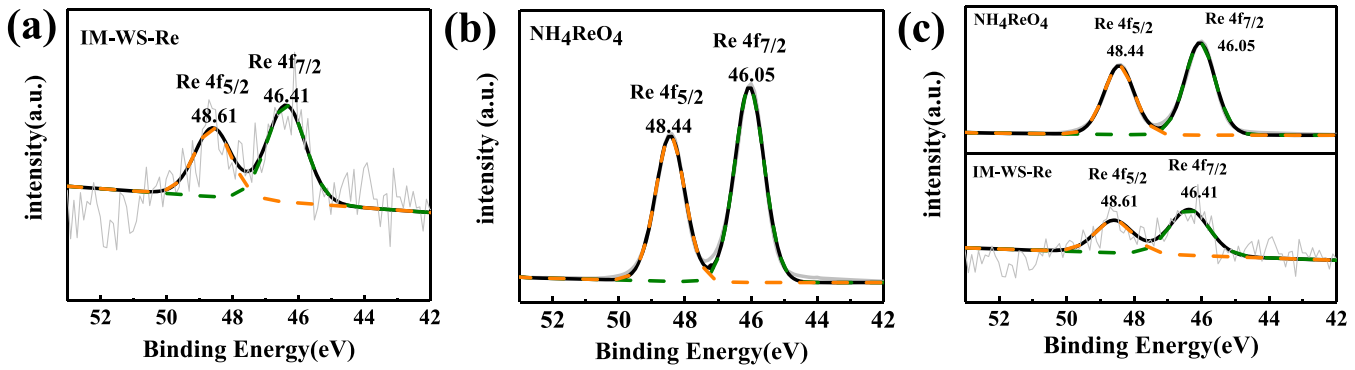

Figure 5. (a) XPS analysis of Re 4f from IM-WS-Re. (b) XPS analysis of Re 4f from NH_4ReO_4. (c) XPS analysis of Re 4f from IM-WS-Re and NH_4ReO_4.

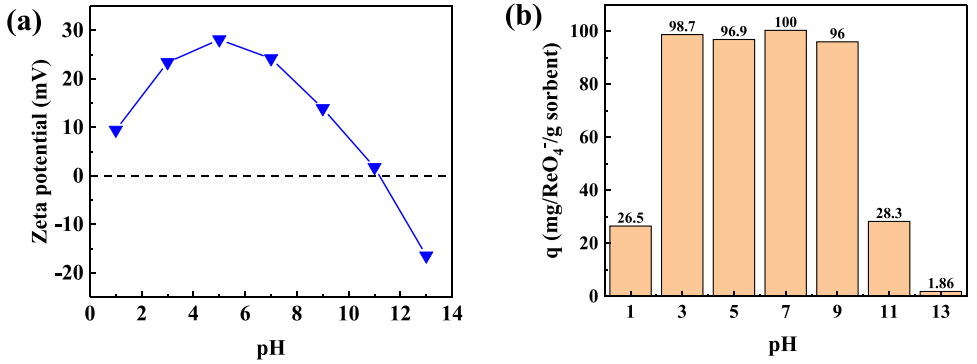

Figure 6. (a) Effect of pH on ζ-potential of IM-WS. (b) Effect of pH on the sorption properties of ReO_4^- by IM-WS.

sample IM-WS-Re was collected, washed three times with water, and dried under vacuum.

Comparing the FT-IR spectra of IM-WS-Re with those of IM-WS (Figure 2), there is a significant new peak at 907 cm^{-1}, which is attributed to the Re−O $\nu 3$ asymmetric stretch. The EDS spectrum of IM-WS-Re (Figure S2) confirms the successful uptake of ReO_4^-. Compared to the EDS mappings of IM-WS and IM-WS-Re (Figure 1d), we can find that the amount of Cl has an appreciable decrease after Re uptake. The X-ray photoelectron spectroscopy (XPS) analysis result (Figure 5a) confirms that the oxidation state of Re(VII) was unchanged after adsorption, indicating that the Re species in IM-WS-Re is perrhenate. On comparing the XPS results of IM-WS-Re with those of NH_4ReO_4 (Figure 5c), the shifts of Re $4f_{5/2}$ and $4f_{5/7}$ are 0.17 and 0.36 eV, respectively, indicating that there are special interactions between ReO_4^- and the imidazolium cation. Combining the above results, we can confirm that the adsorption of ReO_4^- by IM-WS is an anion-exchange process.

2.2.4. pH Effect. ζ-Potentials of IM-WS in different pHs were studied in detail. Typically, 10 mg of IM-WS was added to 5 mL of the aqueous solution, whose pH was adjusted from 1 to 13. It was stirred for 12 h at room temperature. IM-WS was separated for the ζ-potential test. IM-WS shows a positive ζ-potential in the range of pH 1−11 (Figure 6a), indicating that the surface of the material is positively charged. As shown in Figure 6b, the adsorption capacity of IM-WS for ReO_4^- remains almost unchanged for pH 3−9 and decreases when pH > 9 and pH < 3. IM-WS has good adsorption stability over a wide pH range from 3 to 9, which is necessary for practical applications in polluted sewage treatment (pH 8.0−8.5) during nuclear accidents. The adsorption capacity decreases when pH

https://doi.org/10.1021/acsomega.1c03784
ACS Omega 2021, 6, 25672−25679

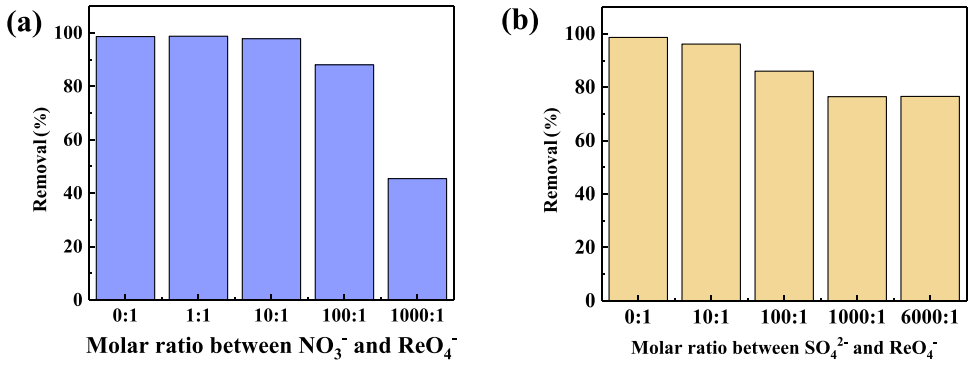

Figure 7. (a) Effect of competing NO_3^- on adsorption of ReO_4^- by IM-WS. (b) Effect of competing SO_4^{2-} on adsorption of ReO_4^- by IM-WS.

> 9 and pH < 3, indicating that both H^+ and HO^- have an effect on the adsorption capacity.

2.2.5. Uptake Selectivity. Considering that there are many kinds of anions in radioactive waste solutions, it is necessary to investigate the adsorption selectivity of IM-WS for TcO_4^-. The adsorption properties of IM-WS toward ReO_4^- were further studied in the presence of different excesses of NO_3^- and SO_4^{2-}. The results are shown in Figure 7a,b. It can be seen that with molar ratios of NO_3^-/ReO_4^- = 1000:1 and SO_4^{2-}/ReO_4^- = 6000:1, the removal efficiency for ReO_4^- can reach 45.44 and 76.57%, respectively. The result is similar to that of imidazolium-based cationic polymer materials SCU-CPN-1[30] and ImPOP-1.[29] The standard Gibbs energy of hydration of ReO_4^- is −330 kJ mol^{-1}, which is close to that of NO_3^- (−306 kJ mol^{-1}) but much lower than that of SO_4^{2-} (−1090 kJ mol^{-1}), which can explain the fact that NO_3^- has a greater competitive effect on the removal of ReO_4^- than SO_4^{2-}.[15,42,43] The selectivity for ReO_4^- in the presence of NO_3^- may be due to the special interactions between tetrahedral ReO_4^-/TcO_4^- anions and the imidazolium cation.

When the concentration of coexisting SO_4^{2-} is 1000 times that of TcO_4^-, after adsorption, the concentration of TcO_4^- decreased to 0.056 ppb from the initial concentration of 12.09 ppb (Table 2). The removal rate reached 99.54%, indicating the potential of treating trace technetium with IM-WS.

Table 2. Trace Technetium Adsorption Result

C_0 (TcO_4^-) (ppb)	C_e (TcO_4^-) (ppb)	solid/liquid ratio (g L^{-1})	molar ratio between SO_4^{2-} and TcO_4^-	removal (%)
12.09	0.056	20	1000	99.54

2.2.6. Simulated Nuclear Wastes. The separation ability of IM-WS toward TcO_4^- in simulated low-level radioactive wastewater was tested. The chemical composition of simulated wastewater containing Tc is shown in Table 3. The concentrations of NO_3^- and Cl^- in the solution were more than 300 times that of TcO_4^-/ReO_4^-. The excess of NO_2^- was even more than 800 times that of TcO_4^-/ReO_4^- (Table 3). The adsorption efficiency to Tc was 92.2% and to Re was 88.3% at the solid/liquid ratio of 50 g L^{-1} (Figure 8 and Table S3). The better removal of Tc % and Re % is due to the lower Gibbs energy of hydration of TcO_4^- (−251 kJ mol^{-1}) and ReO_4^- (−330 kJ mol^{-1}) and the special interactions between tetrahedral TcO_4^-/ReO_4^- anions and the imidazolium cation. These data show the excellent selectivity of IM-WS toward TcO_4^- and the practical application potential of IM-WS in nuclear waste treatment.

Table 3. Composition of Simulated Mixed Solution

anions	concentration (mol L^{-1})	anion/ReO_4^- molar ratio
TcO_4^- or ReO_4^-	1.94×10^{-4}	
NO_3^-	6.07×10^{-2}	314
Cl^-	6.39×10^{-2}	330
NO_2^-	1.69×10^{-1}	873
SO_4^{2-}	6.64×10^{-6}	0.0343
CO_3^{2-}	4.30×10^{-5}	0.222

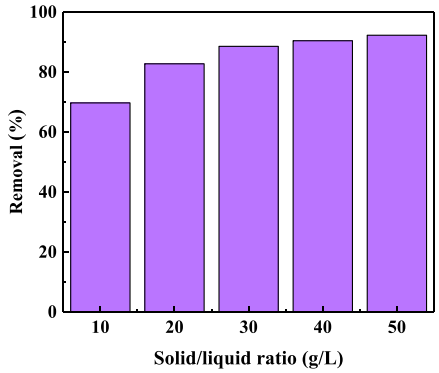

Figure 8. (a) Removal of TcO_4^- in simulated nuclear wastes with different solid/liquid ratios.

3. CONCLUSIONS

We describe the application of imidazolium-functionalized natural wood sawdust as an anion-exchange material for adsorption of ReO_4^-/TcO_4^-. It is observed that the functionalized wood sawdust bearing imidazolium groups is a highly efficient anion-exchange material that has fast adsorption dynamics and high adsorption capacity. Anions with low charge density, such as ReO_4^-/TcO_4^- or NO_3^-, display a higher affinity toward the immobilized imidazolium species. Our work shows that natural sawdust can not only be developed into a material with the strength of the anion-exchange resin but also improve the mass transfer properties that may lead to more efficient separations. This work reports the first example of wood-functionalized materials showing application in purification of radioactive wastewater and provides a new design philosophy for biomass materials for the remediation of environment in the future.

https://doi.org/10.1021/acsomega.1c03784
ACS Omega 2021, 6, 25672−25679

4. EXPERIMENTAL SECTION

4.1. Materials and Chemicals. All reagents and solvents were obtained commercially and used as received. The wood sawdust was purchased from Changzhou, Jiangsu. 1,1′-(1,4-butanediyl)diimidazole was synthesized according to previously reported steps.[44]

4.2. Adsorbent Synthesis. *4.2.1. Synthesis of Cl-WS.* The natural wood sawdust was washed with distilled water to remove impurities and dried. Then, wood sawdust (1.04 g), chloroacetyl chloride (5.73 mL), Na_2CO_3 (0.6 g), and CH_2Cl_2 (80 mL) were mixed and stirred at 50 °C under reflux for 3 days. The mixture was filtered, washed three times with water and methanol successively, and dried under vacuum to obtain Cl-WS.

4.2.2. Synthesis of IM-WS. Cl-WS (0.5 g), 1,1′-(1,4-butanediyl)diimidazole (0.3628 g), and tetrahydrofuran (THF) (50 mL) were mixed and stirred at 90 °C under reflux for 3 days. The mixture was filtered, washed three times with water and methanol successively, and dried under vacuum to obtain the imidazolium-functionalized wood sawdust (IM-WS).

4.3. Sorption Tests. *4.3.1. Sorption Kinetic Tests.* First, 10 mg of IM-WS was added to 5 mL of an aqueous solution containing 100 ppm ReO_4^-, which had been adjusted to pH 7. The mixture was stirred at 25 °C for 30 s and 1, 2, 5, 10, 20, 40, 60, 90, and 120 min, successively. Then, the samples were separated for inductively coupled plasma-optical emission spectrometry (ICP-OES) analysis. The adsorption capacity (q_t, mg g^{-1}) of IM-WS toward ReO_4^- at contact time t was calculated according to eq 2

$$q_t = \frac{(C_0 - C_t)V}{m} \tag{2}$$

where C_0 and C_t are the concentrations of the ReO_4^- solution (mg L^{-1}) initially and at time t, respectively, m is the mass of the absorbent (g), and V is the volume of the solution (L).

The pseudo-first-order and pseudo-second-order kinetic models were used to analyze the adsorption kinetic data. The linearization forms of the two models are shown in eqs 3 and 4, respectively.

Pseudo-first-order model:

$$\ln(q_e - q_t) = \ln q_e - k_1 t \tag{3}$$

Pseudo-second-order model:

$$\frac{t}{q_t} = \frac{1}{k_2 q_e^2} + \frac{t}{q_e} \tag{4}$$

where q_e and q_t represent the adsorption capacity of ReO_4^- (mg g^{-1}) at equilibrium and at contact time t (min), respectively, and k_1 (min^{-1}) and k_2 (g mg^{-1} min^{-1}) are the rate constants of the pseudo-first-order and pseudo-second-order equations, respectively.

4.3.2. Sorption Isotherm Tests. Briefly, 10 mg of IM-WS was added to 5 mL of ReO_4^- aqueous solution, which had been adjusted to pH 7. The initial concentrations of ReO_4^- were varied from 100 to 1500 ppm. The solution was stirred for 12 h at 25 °C. The supernatant was separated for ICP-OES analysis.

The classical Langmuir[45] and Freundlich models were used to analyze the adsorption isotherm data. The linearization forms of the two models are eqs 5 and 6, respectively.

Langmuir model:

$$\frac{C_e}{q_e} = \frac{1}{q_m K_L} + \frac{C_e}{q_m} \tag{5}$$

Freundlich model:

$$\ln q_e = \ln K_F + \frac{1}{n} \ln C_e \tag{6}$$

where q_e and q_m are the adsorption capacity at equilibrium and the maximum adsorption capacity of IM-WS toward ReO_4^- (mg g^{-1}), respectively. C_e is the concentration of ReO_4^- in the solution (mg L^{-1}) at equilibrium. K_L (L mg^{-1}) is the Langmuir constant related to adsorption capacity and energy. K_F and n are the Freundlich parameters related to adsorption capacity and adsorption intensity, respectively.

4.3.3. pH Effect Tests. Overall, 10 mg of IM-WS was added to 5 mL of an aqueous solution containing 200 ppm ReO_4^-, whose pH was adjusted from 1 to 13 using HNO_3 and NaOH solutions. After being stirred for 12 h at room temperature, the resulting mixture was separated for ICP-OES analysis.

4.3.4. Uptake Selectivity Tests. Briefly, 10 mg of IM-WS was added to 5 mL of an aqueous solution containing 0.05 mM ReO_4^- and different concentrations of $NaNO_3$ (0.05, 0.5, 5, and 50 mM) or Na_2SO_4 (0.005, 0.05, 0.5, 5, 50, and 300 mM) to test the selectivity of IM-WS toward ReO_4^- among the competing ions. The solution was stirred for 12 h at 25 °C, and the resulting mixture was separated for ICP-OES analysis.

4.3.5. Simulated Nuclear Wastes Tests. The simulated mixed solution was prepared as per the reported protocol.[46] The concentrations of TcO_4^- or ReO_4^-, NO_3^-, Cl^-, NO_2^-, SO_4^{2-}, and CO_3^{2-} anions were 1.94×10^{-4}, 6.07×10^{-2}, 6.39×10^{-2}, 1.69×10^{-1}, 6.64×10^{-6}, and 4.30×10^{-5} mol L^{-1}, respectively (Table 1).

To test the selectivity of IM-WS toward TcO_4^- or ReO_4^-, 10, 20, 30, 40, and 50 mg of IM-WS were added to 1 mL of the above simulated nuclear waste solutions. After being stirred for 12 h, the samples were separated and Tc was monitored by liquid scintillation counting measurements.

4.3.6. Trace Technetium Adsorption Tests. For tests, 20 mg of IM-WS was added to 1 mL of an aqueous solution containing 12.09 ppb TcO_4^-, and the concentration of SO_4^{2-} was 1000 times that of TcO_4^-. After being stirred for 12 h at 25 °C, the supernatant liquid was separated for ICP-MS analysis.

Safety Notes. ^{99}Tc is β-emitter (E_{max} = 294 keV, $t_{1/2}$=2 ×10^5 years). All operations were carried out in radiochemical laboratories equipped for handling this isotope.

■ ASSOCIATED CONTENT

Supporting Information

The Supporting Information is available free of charge at https://pubs.acs.org/doi/10.1021/acsomega.1c03784.

Element content from EDS in WS, Cl-WS, IM-WS, and IM-WS-Re (Table S1); SEM images of WS and Cl-WS (Figure S1); EDS spectrum of IM-WS-Re (Figure S2); adsorption parameters of ReO_4^- by IM-WS (Table S2); and results of ReO_4^- sorption by IM-WS from simulated nuclear wastes (Table S3) (PDF)

https://doi.org/10.1021/acsomega.1c03784
ACS Omega 2021, 6, 25672−25679

AUTHOR INFORMATION

Corresponding Authors

Suliang Yang − *Radiochemistry Department, China Institute of Atomic Energy, Beijing 102413, China*; Email: ysl79@hotmail.com

Yinglin Shen − *School of Nuclear Science and Technology, Lanzhou University, Lanzhou 730000, China*; orcid.org/0000-0002-7317-797X; Email: shenyl@lzu.edu.cn

Authors

Fangfei Dong − *School of Nuclear Science and Technology, Lanzhou University, Lanzhou 730000, China*

Xiaomin Li − *School of Nuclear Science and Technology, Lanzhou University, Lanzhou 730000, China*

Yiwei Huang − *School of Nuclear Science and Technology, Lanzhou University, Lanzhou 730000, China*

Xupeng Zhi − *School of Nuclear Science and Technology, Lanzhou University, Lanzhou 730000, China*

Complete contact information is available at: https://pubs.acs.org/10.1021/acsomega.1c03784

Notes

The authors declare no competing financial interest.

ACKNOWLEDGMENTS

This work was supported by the National Natural Science Foundation of China (21976075).

REFERENCES

(1) Icenhower, J. P.; Qafoku, N. P.; Zachara, J. M.; Martin, W. J. The Biogeochemistry of Technetium: A Review of the Behavior of an Artificial Element in the Natural Environment. *Am. J. Sci.* **2010**, *310*, 721−752.

(2) Momoshima, N.; Sayad, M.; Yamada, M.; Takamura, M.; Kawamura, H. Global fallout levels of Tc-99 and activity ratio of Tc-99/Cs-137 in the Pacific Ocean. *J. Radioanal. Nucl. Chem.* **2005**, *266*, 455−460.

(3) Radivojevic Jovanovic, I.; Gallagher, C. M. B.; Salcedo, R.; Lukens, W. W.; Burton-Pye, B. P.; McGregor, D.; Francesconi, L. C. Strategies for the Photoreduction of Tc-99 Pertechnetate to Low-Valent Tc by Keggin Polyoxometalates. *Eur. J. Inorg. Chem.* **2020**, *2020*, 2133−2142.

(4) McBeth, J. M.; Lear, G.; Lloyd, J. R.; Livens, F. R.; Morris, K.; Burke, I. T. Technetium reduction and reoxidation in aquifer sediments. *Geomicrobiol. J.* **2007**, *24*, 189−197.

(5) Um, W.; Chang, H.; Icenhower, J. P.; Lukens, W. W.; Serne, R. J.; Qafoku, N.; Kukkadapu, R. K.; Westsik, J. H. Iron oxide waste form for stabilizing (TC)-T-99. *J. Nucl. Mater.* **2012**, *429*, 201−209.

(6) Um, W.; Chang, H. S.; Icenhower, J. P.; Lukens, W. W.; Serne, R. J.; Qafoku, N. P.; Westsik, J. H.; Buck, E. C.; Smith, S. C. Immobilization of 99-Technetium (VII) by Fe(II)-Goethite and Limited Reoxidation. *Environ. Sci. Technol.* **2011**, *45*, 4904−4913.

(7) Choi, J.; Um, W.; Choung, S. Development of iron phosphate ceramic waste form to immobilize radioactive waste solution. *J. Nucl. Mater.* **2014**, *452*, 16−23.

(8) Levitskaia, T. G.; Chatterjee, S.; Pence, N. K.; Romero, J.; Varga, T.; Engelhard, M. H.; Du, Y. G.; Kovarik, L.; Arey, B. W.; Bowden, M. E.; Walter, E. D. Inorganic tin aluminophosphate nanocomposite for reductive separation of pertechnetate. *Environ. Sci.: Nano* **2016**, *3*, 1003−1013.

(9) Bishop, M. E.; Dong, H. L.; Kukkadapu, R. K.; Liu, C. X.; Edelmann, R. E. Bioreduction of Fe-bearing clay minerals and their reactivity toward pertechnetate (Tc-99). *Geochim. Cosmochim. Acta* **2011**, *75*, 5229−5246.

(10) Liu, Y.; Terry, J.; Jurisson, S. Pertechnetate immobilization in aqueous media with hydrogen sulfide under anaerobic and aerobic environments. *Radiochim. Acta* **2007**, *95*, 717−725.

(11) Liu, Y.; Terry, J.; Jurisson, S. S. Potential interferences on the pertechnetate-sulfide immobilization reaction. *Radiochim. Acta* **2009**, *97*, 33−41.

(12) Liu, Y.; Terry, J.; Jurisson, S. Pertechnetate immobilization with amorphous iron sulfide. *Radiochim. Acta* **2008**, *96*, 823−833.

(13) Zhu, L.; Xiao, C. L.; Dai, X.; Li, J.; Gui, D. X.; Sheng, D. P.; Chen, L. H.; Zhou, R. H.; Chai, Z. F.; Albrecht-Schmitt, T. E.; Wang, S. Exceptional Perrhenate/Pertechnetate Uptake and Subsequent Immobilization by a Low-Dimensional Cationic Coordination Polymer: Overcoming the Hofmeister Bias Selectivity. *Environ. Sci. Technol. Lett.* **2017**, *4*, 316−322.

(14) Custelcean, R. Urea-functionalized crystalline capsules for recognition and separation of tetrahedral oxoanions. *Chem. Commun.* **2013**, *49*, 2173−2182.

(15) Custelcean, R.; Moyer, B. A. Anion separation with metal-organic frameworks. *Eur. J. Inorg. Chem.* **2007**, *10*, 1321−1340.

(16) Darab, J. G.; Smith, P. A. Chemistry of technetium and rhenium species during low-level radioactive waste vitrification. *Chem. Mater.* **1996**, *8*, 1004−1021.

(17) Katayev, E. A.; Kolesnikov, G. V.; Sessler, J. L. Molecular recognition of pertechnetate and perrhenate. *Chem. Soc. Rev.* **2009**, *38*, 1572−1586.

(18) Banerjee, D.; Kim, D.; Schweiger, M. J.; Kruger, A. A.; Thallapally, P. K. Removal of TcO4- ions from solution: materials and future outlook. *Chem. Soc. Rev.* **2016**, *45*, 2724−2739.

(19) Wang, S. A.; Alekseev, E. V.; Juan, D. W.; Casey, W. H.; Phillips, B. L.; Depmeier, W.; Albrecht-Schmitt, T. E. NDTB-1: A Supertetrahedral Cationic Framework That Removes TcO4- from Solution. *Angew. Chem., Int. Ed.* **2010**, *49*, 1057−1060.

(20) Goh, K. H.; Lim, T. T.; Dong, Z. Application of layered double hydroxides for removal of oxyanions: A review. *Water Res.* **2008**, *42*, 1343−1368.

(21) Wilmarth, W. R.; Lumetta, G. J.; Johnson, M. E.; Poirier, M. R.; Thompson, M. C.; Suggs, P. C.; Machara, N. P. Review: Waste-Pretreatment Technologies for Remediation of Legacy Defense Nuclear Wastes. *Solvent Extr. Ion Exch.* **2011**, *29*, 1−48.

(22) Wang, Y. F.; Gao, H. Z. Compositional and structural control on anion sorption capability of layered double hydroxides (LDHs). *J. Colloid Interface Sci.* **2006**, *301*, 19−26.

(23) Gándara, F.; Perles, J.; Snejko, N.; Iglesias, M.; Gomez-Lor, B.; Gutierrez-Puebla, E.; Monge, M. A. Layered rare-earth hydroxides: A class of pillared crystalline compounds for intercalation chemistry. *Angew. Chem., Int. Ed.* **2006**, *45*, 7998−8001.

(24) Sheng, D. P.; Zhu, L.; Xu, C.; Xiao, C. L.; Wang, Y. L.; Wang, Y. X.; Chen, L. H.; Diwu, J.; Chen, J.; Chai, Z. F.; Albrecht-Schmitt, T. E.; Wang, S. A. Efficient and Selective Uptake of TcO4- by a Cationic Metal-Organic Framework Material with Open Ag+ Sites. *Environ. Sci. Technol.* **2017**, *51*, 3471−3479.

(25) Fei, H. H.; Bresler, M. R.; Oliver, S. R. J. A New Paradigm for Anion Trapping in High Capacity and Selectivity: Crystal-to-Crystal Transformation of Cationic Materials. *J. Am. Chem. Soc.* **2011**, *133*, 11110−11113.

(26) Liu, X.; Pang, H.; Liu, X.; Li, Q.; Zhang, N.; Mao, L.; Qiu, M.; Hu, B.; Yang, H.; Wang, X. Orderly Porous Covalent Organic Frameworks-based Materials: Superior Adsorbents for Pollutants Removal from Aqueous Solutions. *Innovation* **2021**, *2*, No. 100076.

(27) He, L. W.; Liu, S. T.; Chen, L.; Dai, X.; Li, J.; Zhang, M. X.; Ma, F. Y.; Zhang, C.; Yang, Z. X.; Zhou, R. H.; Chai, Z. F.; Wang, S. Mechanism unravelling for ultrafast and selective (TcO4-)-Tc-99 uptake by a radiation-resistant cationic covalent organic framework: a combined radiological experiment and molecular dynamics simulation study. *Chem. Sci.* **2019**, *10*, 4293−4305.

(28) Wang, X. X.; Chen, L.; Wang, L.; Fan, Q. H.; Pan, D. Q.; Li, J. X.; Chi, F. T.; Xie, Y.; Yu, S. J.; Xiao, C. L.; Luo, F.; Wang, J.; Wang, X. L.; Chen, C. L.; Wu, W. S.; Shi, W. Q.; Wang, S.; Wang, X. K.

Synthesis of novel nanomaterials and their application in efficient removal of radionuclides. *Sci. China: Chem.* **2019**, *62*, 933−967.
(29) Liu, Z. W.; Han, B. H. Evaluation of an Imidazolium-Based Porous Organic Polymer as Radioactive Waste Scavenger. *Environ. Sci. Technol.* **2020**, *54*, 216−224.
(30) Li, J.; Dai, X.; Zhu, L.; Xu, C.; Zhang, D.; Silver, M. A.; Li, P.; Chen, L.; Li, Y.; Zuo, D.; Zhang, H.; Xiao, C.; Chen, J.; Diwu, J.; Farha, O. K.; Albrecht-Schmitt, T. E.; Chai, Z.; Wang, S. 99TcO4(-) remediation by a cationic polymeric network. *Nat. Commun.* **2018**, *9*, No. 3007.
(31) Guo, R. X.; Cai, X. H.; Liu, H. W.; Yang, Z.; Meng, Y. J.; Chen, F. J.; Li, Y. J.; Wang, B. D. In Situ Growth of Metal-Organic Frameworks in Three-Dimensional Aligned Lumen Arrays of Wood for Rapid and Highly Efficient Organic Pollutant Removal. *Environ. Sci. Technol.* **2019**, *53*, 2705−2712.
(32) Liu, G. G.; Chen, D. Y.; Liu, R. K.; Yu, Z. Y.; Jiang, J. L.; Liu, Y.; Hu, J. B.; Chang, S. S. Antifouling Wood Matrix with Natural Water Transfer and Microreaction Channels for Water Treatment. *ACS Sustainable Chem. Eng.* **2019**, *7*, 6782−6791.
(33) Chen, F. J.; Gong, A. S.; Zhu, M. W.; Chen, G.; Lacey, S. D.; Jiang, F.; Li, Y. F.; Wang, Y. B.; Dai, J. Q.; Yao, Y. G.; Song, J. W.; Liu, B. Y.; Fu, K.; Das, S.; Hu, L. B. Mesoporous, Three-Dimensional Wood Membrane Decorated with Nanoparticles for Highly Efficient Water Treatment. *ACS Nano* **2017**, *11*, 4275−4282.
(34) Guo, R. X.; Liu, H. W.; Yang, K.; Wang, S. T.; Sun, P. P.; Gao, H.; Wang, B. D.; Chen, F. J. beta-Cyclodextrin Polymerized in Cross-Flowing Channels of Biomass Sawdust for Rapid and Highly Efficient Pharmaceutical Pollutants Removal from Water. *ACS Appl. Mater. Interfaces* **2020**, *12*, 32817−32826.
(35) Gu, Y.; Ye, M. X.; Wang, Y. C.; Li, H. M.; Zhang, H. M.; Wang, G. Z.; Zhang, Y. X.; Zhao, H. J. Lignosulfonate functionalized g-C3N4/carbonized wood sponge for highly efficient heavy metal ion scavenging. *J. Mater. Chem. A* **2020**, *8*, 12687−12698.
(36) Yang, Z.; Liu, H. W.; Li, J.; Yang, K.; Zhang, Z. Z.; Chen, F. J.; Wang, B. D. High-Throughput Metal Trap: Sulfhydryl-Functionalized Wood Membrane Stacks for Rapid and Highly Efficient Heavy Metal Ion Removal. *ACS Appl. Mater. Interfaces* **2020**, *12*, 15002−15011.
(37) Bonnesen, P. V.; Brown, G. M.; Alexandratos, S. D.; Bavoux, L. B.; Presley, D. J.; Patel, V.; Ober, R.; Moyer, B. A. Development of bifunctional anion-exchange resins with improved selectivity and sorptive kinetics for pertechnetate: Batch-equilibrium experiments. *Environ. Sci. Technol.* **2000**, *34*, 3761−3766.
(38) Zhu, L.; Sheng, D. P.; Xu, C.; Dai, X.; Silver, M. A.; Li, J.; Li, P.; Wang, Y. X.; Wang, Y. L.; Chen, L. H.; Xiao, C. L.; Chen, J.; Zhou, R. H.; Zhang, C.; Farha, O. K.; Chai, Z. F.; Albrecht-Schmitt, T. E.; Wang, S. Identifying the Recognition Site for Selective Trapping of (TcO4-)-Tc-99 in a Hydrolytically Stable and Radiation Resistant Cationic Metal-Organic Framework. *J. Am. Chem. Soc.* **2017**, *139*, 14873−14876.
(39) Sheng, D. P.; Zhu, L.; Dai, X.; Xu, C.; Li, P.; Pearce, C. I.; Xiao, C. L.; Chen, J.; Zhou, R. H.; Duan, T.; Farha, O. K.; Chai, Z. F.; Wang, S. Successful Decontamination of (TcO4-)-Tc-99 in Groundwater at Legacy Nuclear Sites by a Cationic Metal-Organic Framework with Hydrophobic Pockets. *Angew. Chem., Int. Ed.* **2019**, *58*, 4968−4972.
(40) Shen, N.; Yang, Z.; Liu, S.; Dai, X.; Xiao, C.; Taylor-Pashow, K.; Li, D.; Yang, C.; Li, J.; Zhang, Y.; Zhang, M.; Zhou, R.; Chai, Z.; Wang, S. 99TcO4(-) removal from legacy defense nuclear waste by an alkaline-stable 2D cationic metal organic framework. *Nat. Commun.* **2020**, *11*, No. 5571.
(41) Sun, Q.; Zhu, L.; Aguila, B.; Thallapally, P. K.; Xu, C.; Chen, J.; Wang, S.; Rogers, D.; Ma, S. Optimizing radionuclide sequestration in anion nanotraps with record pertechnetate sorption. *Nat. Commun.* **2019**, *10*, No. 1646.
(42) Xiao, C. L.; Khayambashi, A.; Wang, S. Separation and Remediation of (TcO4-)-Tc-99 from Aqueous Solutions. *Chem. Mater.* **2019**, *31*, 3863−3877.
(43) Dickson, J. O.; Harsh, J. B.; Lukens, W. W.; Pierce, E. M. Perrhenate incorporation into binary mixed sodalites: The role of anion size and implications for technetium-99 sequestration. *Chem. Geol.* **2015**, *395*, 138−143.
(44) Daneshvar, N.; Nasiri, M.; Shirzad, M.; Langarudi, M. S. N.; Shirini, F.; Tajik, H. The introduction of two new imidazole-based bis-dicationic Bronsted acidic ionic liquids and comparison of their catalytic activity in the synthesis of barbituric acid derivatives. *New J. Chem.* **2018**, *42*, 9744−9756.
(45) Langmuir, I. The Adsorption of Gases on Plane Surfaces of Glass, Mica and Platinum. *J. Am. Chem. Soc.* **1918**, *40*, 1361−1403.
(46) Wang, S. A.; Yu, P.; Purse, B. A.; Orta, M. J.; Diwu, J.; Casey, W. H.; Phillips, B. L.; Alekseev, E. V.; Depmeier, W.; Hobbs, D. T.; Albrecht-Schmitt, T. E. Selectivity, Kinetics, and Efficiency of Reversible Anion Exchange with TcO4- in a Supertetrahedral Cationic Framework. *Adv. Funct. Mater.* **2012**, *22*, 2241−2250.

https://doi.org/10.1021/acsomega.1c03784
ACS Omega 2021, 6, 25672−25679